Clean Energy and Smart Technology
Volume 04, Number 02, April 2026
DOI : https://doi.org/10.58641/
e-ISSN : 2964-2647

STRUCTURAL DESIGN ANALYSIS OF A ROBOTIC AUTOMATED GUIDED VEHICLE (AGV) CHASSIS USING EXPERIMENTAL AND NUMERICAL APPROACHES

Danu Prasetyo[1)], Sunaryo[2*)], Heru Nugroho[3)], Budi Santoso[3)]
[1,2,3,4)] Mechanical Engineering Department, Universitas Sains Al-Qur'an, Indonesia
pdanu1023@email.com[1)], sunaryo@unsiq.ac.id[2)], suheru.st@gmail.com[3)], budisantoso@unsiq.ac.id[4)]
*Corresponding author: sunaryo@unsiq.ac.id

Submitted : 6 April 2026 | **Accepted** : 28 April 2026 | **Published** : 30 April 2026

Abstract: This study presents an integrated experimental–numerical framework to evaluate and compare the structural performance of robotic Automated Guided Vehicle (AGV) chassis using two commonly applied structural steels, ASTM A36 and ASTM A500. The novelty of this work lies in the direct validation of Finite Element Analysis (FEA) results with experimental measurements under controlled loading conditions, enabling a more reliable assessment of stress, deflection, and safety factor for compact AGV chassis designs. A chassis with dimensions of 400 × 300 × 80 mm was analyzed under static loads of 5, 10, and 15 kg. Numerical simulations were performed using FEA, while experimental validation was conducted using a dial indicator to measure deflection.
The results indicate that under a 15 kg load, ASTM A500 exhibits lower maximum stress (60.15 MPa) and deflection (0.78 mm) compared to ASTM A36 (68.06 MPa and 0.89 mm). The discrepancy between numerical and experimental results remains below 10%, confirming the reliability of the proposed approach. In terms of structural safety, ASTM A500 achieves a higher safety factor (2.71) than ASTM A36, indicating superior load-bearing capability and structural stability.
These findings demonstrate that ASTM A500 provides a more efficient and mechanically robust solution for AGV chassis applications. The study contributes a validated methodology for material selection and structural evaluation in AGV design, supporting improved reliability in industrial robotic transportation systems.

Keywords: Optimization, Automated Guide Vehicle, Design, Robots

1. INTRODUCTION

Automated Guided Vehicles (AGVs) have become a key component of modern industrial automation, particularly in manufacturing and logistics systems, due to their ability to transport materials autonomously and improve operational efficiency (Krnjak et al., 2015; Setiawan et al., 2023). The chassis is a critical structural element of an AGV, as it supports all onboard components and payloads. Consequently, its structural integrity directly affects system stability, reliability, and operational safety under varying loading conditions (Oyekanlu et al., 2020).

The structural performance of an AGV chassis is strongly influenced by material selection, in addition to geometric configuration and manufacturing processes. Therefore, accurate evaluation of stress, deformation, and safety factors is essential during the design stage (Kurniawan, 2022). Previous studies have demonstrated that both experimental testing and numerical methods are effective approaches for assessing structural behavior under

Clean Energy and Smart Technology
Volume 04, Number 02, April 2026
DOI : https://doi.org/10.58641/
e-ISSN : 2964-2647

loading conditions (Haryanto et al., 2022). However, many studies tend to rely predominantly on numerical simulations without sufficient experimental validation, which may limit the reliability of the predicted results.

Among commonly used structural materials, ASTM A36 and ASTM A500 steels are widely applied in light to medium-duty mechanical systems. ASTM A36 is a low-carbon steel known for its good weldability, formability, and cost-effectiveness, making it suitable for general structural applications (Bhavikatti, 2005). In contrast, ASTM A500 offers higher yield strength and stiffness, providing better resistance to deformation under higher loads (Versteeg and Malalasekera, 2007). Despite their widespread use, a direct and experimentally validated comparison of these materials in compact AGV chassis applications remains limited in the literature.

This study aims to address this gap by conducting a comparative structural analysis of ASTM A36 and ASTM A500 for AGV chassis applications using an integrated experimental and Finite Element Analysis (FEA) approach. The novelty of this work lies in the direct validation of numerical results through experimental measurements under controlled loading conditions. This approach enables a more reliable assessment of stress distribution, deflection, and safety factor, thereby providing a stronger basis for material selection in AGV chassis design.

2. MATERIALS AND METHOD

Design of Automated Guided Vehicles

This design features a six-wheel chassis structure, consisting of two differential wheels located in the center and four universal wheels at the front and rear. With dimensions of 400 mm in length, 300 mm in width, and 80 mm in height when closed and 217.77 mm when raised, it was designed using CAD software with consideration of fatigue criteria and then analyzed through a numerical study using the FEA method; the chassis geometry is shown in Figure 1. In the chassis design, material selection must be tailored to requirements without neglecting aspects such as quality, production time, and ease of assembly. The AGV chassis manufacturing process includes: material cutting, grinding, drilling, welding, filling, sanding, painting, and concludes with chassis assembly.

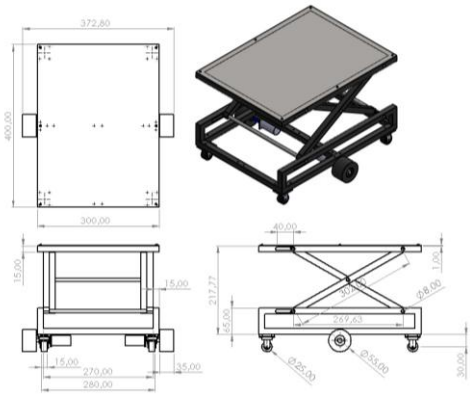

Figure 1. Design of Chassis AGV

Table 1. Mechanical properties of AGV materials

No.	Materials parameter	ASTM A36	ASTM A500
1	Density	7850 Kg/m³	7850 Kg/m³
2	Modulus Elastisity	200 GPa	210 Gpa
3	Poisson's Ratio	0.26	0.30
4	Tensile Strength	550 MPa	400 MPa
5	Yield Strength	250 MPa	290 MPa
6	Elongation	20%	25%

The study was conducted on AGV chassis structures made of two types of structural steel: ASTM A36 and ASTM A500. ASTM A36 is a low-carbon steel with good mechanical properties and weldability, while ASTM A500 is a structural steel with higher yield strength and better resistance to deflection. The mechanical properties of the materials are shown in Table 1.

Clean Energy and Smart Technology
Volume 04, Number 02, April 2026
DOI : https://doi.org/10.58641/
e-ISSN : 2964-2647

Experimental study

This study began with the fabrication of an AGV robot chassis using ASTM A36 and ASTM A500 materials, followed by the assembly of mechanical components. After assembly, load tests were conducted with varying masses to evaluate structural strength, followed by deflection measurements using a dial indicator. The experimental data were compared with the results of numerical simulations based on the Finite Element Analysis (FEA) method, which included modeling, meshing, and validation to predict the structural response to loading. In this test, a dial indicator was used because it has a higher level of precision compared to other measuring instruments, allowing for accurate measurement of small changes in the chassis. The dial indicator was placed in the center of the chassis, specifically on the flat part of the upper support, to accurately measure the changes that occurred during the test. This can be seen in Figure 2.

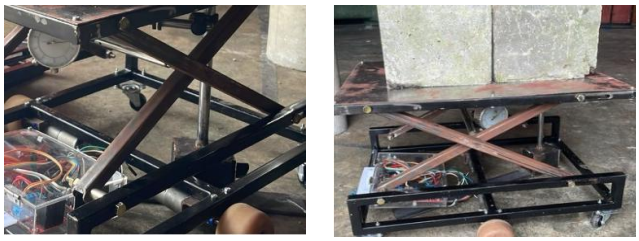

a b

Figure 2. (a) The process of setting up the dial indicator, and (b) The testing process

Numerical study

In Figure 3, a numerical study is the process of simulating the real-world conditions of a system to analyze its performance mathematically (Kresna, Suprapto, and Nendra Wibawa, 2021). Before conducting a numerical study, several important steps are carried out, such as defining the computational domain to convert the AGV geometry into a discrete model using the FEA method. This stage aims to identify areas with high stress or deflection concentrations that could potentially cause structural failure. This demonstrates that proper numerical modeling, with appropriate geometry and computational domain, can provide accurate predictions of the mechanical system's response under specific operating conditions. Boundary conditions were defined by applying cylindrical supports at the wheel mounting points, restricting movement in all axes, and applying a vertical compressive force (Y-direction) to the chassis platform with load variations of 5 kg (49.05 N), 10 kg (98.1 N), and 15 kg (147.15 N).

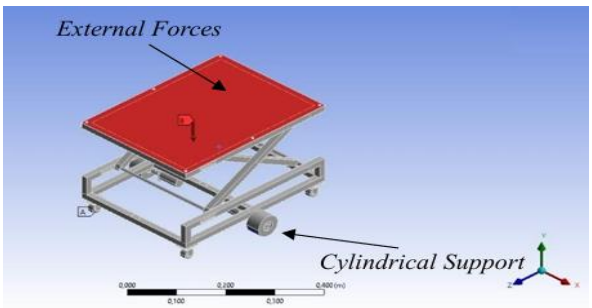

Figure 3. Computational domain and definition of boundary conditions on the AGV chassis geometry

After defining the computational domain, the next step in the numerical study is the meshing process, as shown in Figure 4, which involves discretizing the geometric model into small elements that can be analyzed using the Finite Element Analysis (FEA) method. This step is crucial as it affects the accuracy and stability of simulation results, particularly when analyzing the mechanical behavior of the AGV chassis structure under various loading conditions. The meshing process is performed not only to divide the geometry into smaller sections but also to capture the significant effects of the boundary layer on stress distribution, deformation, and local structural response. In this study, mesh quality was evaluated using the Mesh Metric with the Orthogonal Quality parameter, which showed a minimum value of 0.50813 and a maximum of 0.99829, with an average value of 0.76256 and a standard deviation of 0.11895. These values indicate that the mesh quality is at a good level and suitable for use

Clean Energy and Smart Technology
Volume 04, Number 02, April 2026
DOI : https://doi.org/10.58641/
e-ISSN : 2964-2647

in numerical simulations. The mesh topology used is the Tetrahedron type, which is suitable for complex geometric shapes such as the AGV chassis, with a total of 225.120 cells.

$$\sigma = \frac{F}{A} \quad \text{Stress} \tag{1}$$

$$\varepsilon = \frac{\Delta L}{L_0} \quad \text{Strain} \tag{2}$$

$$\delta = \frac{F \cdot L^3}{3EI} \quad \text{Deflection} \tag{3}$$

3. RESULT AND DISCUSSIONS

Grid testing and data validation

A grid test was conducted to determine the most appropriate number of mesh elements for the numerical study. The number of elements analyzed ranged from 51.283, 117.387, 158.654, to 225.120. The comparison results are shown in a graph illustrating the relationship between the number of grid elements and deflection, as presented in Figure 5. Based on the analysis, the relative error between grids 51.283 and 117.387 reached ±25.91%, between 117.387 and 158.654 was ±6.23%, and between 158.654 and 225.120 was ±0.97%. Since the difference in deflection between the two highest grids is very small (0.00027724 m and 0.00027996 m), grid 225.120 is considered optimal and is used in all subsequent AGV Chassis simulations. This finding is consistent with recent finite element-based structural design studies, which emphasize that mesh refinement is essential to balance computational accuracy and simulation efficiency. Liu et al. (2026), for example, demonstrated that an efficient finite element model can reduce computational scale while maintaining high prediction accuracy, provided that the simplified or refined model is validated against experimental or benchmark data.

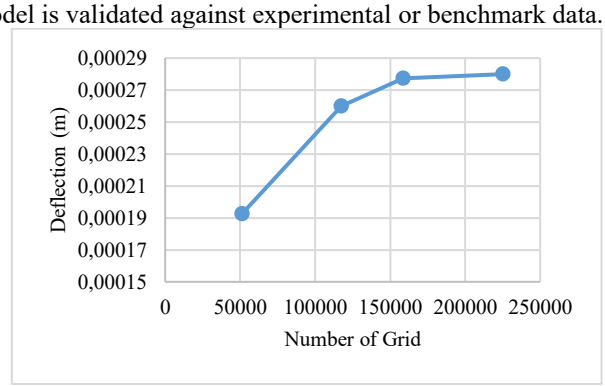

Figure 5. Graph showing the relationship between grid number and deflection

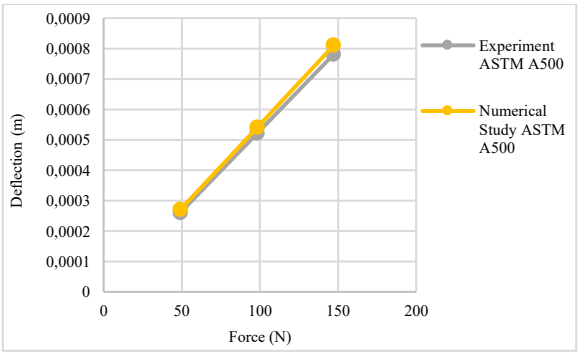

Figure 6. Graph of the force-deflection relationship for ASTM A500 material

Validation was performed to ensure that the results of the FEA numerical study corresponded to real-world conditions by comparing the simulation results with experimental data through variations in force versus deflection on the AGV chassis. For ASTM A36 material, the largest relative error reached 5.25% (experimental: 0.59 mm,

Clean Energy and Smart Technology
Volume 04, Number 02, April 2026
DOI : https://doi.org/10.58641/
e-ISSN : 2964-2647

numerical: 0.55972 mm), and the lowest was 4.12% (experimental: 0.89 mm, numerical: 0.84958 mm). Meanwhile, for ASTM A500, the highest relative error was 3.81% (experimental: 0.00026 mm; numerical: 0.27006 mm), and the lowest was 3.74% (experimental: 0.00078 mm; numerical: 0.80958 mm), as shown in Figure 6. In the present study, the low relative error between experimental and numerical deflection values further supports the reliability of the FEA model for predicting the structural response of the AGV chassis. Similar validation logic was also applied by Rebhi et al. (2025), who combined FEM prediction and laboratory validation to evaluate robotic chassis behavior under random base excitation. Therefore, the agreement between simulation and experimental results strengthens the credibility of the numerical approach used in this research.

The Effect of Load on Stability and Efficiency

Tests to evaluate the effect of load on the stability and efficiency of the AGV chassis structure were conducted using two types of carbon steel, namely ASTM A36 and ASTM A500, with load variations of 5 kg, 10 kg, and 15 kg. The chassis was placed on a flat floor, then a load was gradually applied to the support plate, and deflection was measured using a dial indicator as shown in Figure 7. For ASTM A36, the results showed a linear increase with increasing load, with stresses of 22.69 MPa, 45.38 MPa, and 68.06 MPa, strains of 0.000125 m, 0.0002 m, and 0.000275 m, and deflections of 0.00030 m, 0.00059 m, and 0.00089 m, all still within the elastic limit. For ASTM A500, the recorded stress values were 20.05 MPa, 40.10 MPa, and 60.15 MPa, strains of 0.0001 m, 0.000175 m, and 0.00025 m, and smaller deflections of 0.00026 m, 0.00052 m, and 0.00078 m. This indicates that ASTM A500 has better deflection resistance than ASTM A36, making it more efficient and stable under increased loads.

Figure 7. Load testing on the AGV frame

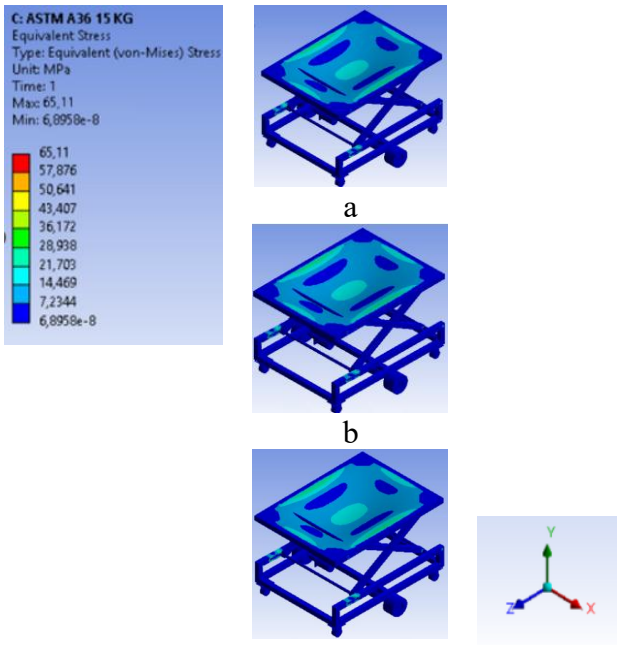

Figure 8. Stress-strain curves for ASTM A36 material: (a) 5 kg load, (b) 10 kg load, and (c) 15 kg load.

Clean Energy and Smart Technology
Volume 04, Number 02, April 2026
DOI : https://doi.org/10.58641/
e-ISSN : 2964-2647

The stress contours shown in Figure 8 from the results of the numerical study using the FEA method indicate that both ASTM A36 and ASTM A500 materials exhibit a linear increase in stress, strain, and deflection with increasing load. For ASTM A36 material, at a load of 5 kg, a stress of 22.69 MPa, a strain of 0.000125 m, and a deflection of 0.00032 m were obtained. When the load was increased to 10 kg, the stress rose to 45.38 MPa, the strain to 0.0002 m, and the deflection to 0.00059 m. At the highest load of 15 kg, the stress reached 68.06 MPa, the strain was 0.000275 m, and the deflection was 0.00084958 m. Meanwhile, for ASTM A500 material, at a load of 5 kg, the stress was 20.85 MPa, the strain was 0.000112 m, and the deflection was 0.00027006 m. At a load of 10 kg, the stress increased to 41.70 MPa, the strain to 0.00018 m, and the deflection to 0.00053992 m. Meanwhile, at a load of 15 kg, the stress reached 62.55 MPa, the strain 0.00024 m, and the deflection 0.00080958 m.

The Effect of Material Type on Stability and Efficiency

Figure 9 shows the relationship between force (N) and stress (MPa) for ASTM A36 and ASTM A500 materials, based on both experimental testing and numerical simulation. ASTM A36 exhibits higher stress than ASTM A500 at every load level. At a load of 15 kg (147.15 N), the maximum stress from the ASTM A36 experimental results reached 68.06 MPa, while that of ASTM A500 was 60.15 MPa. The numerical results show a similar trend: ASTM A36 reached 65.11 MPa, and ASTM A500 was 63.11 MPa. Both materials exhibit a linear pattern and remain within the elastic limit. The higher stress in ASTM A36 indicates a greater modulus of elasticity, but also the potential for higher internal stress accumulation. Conversely, ASTM A500 offers better structural stiffness and flexibility, making it the superior choice in terms of long-term durability.

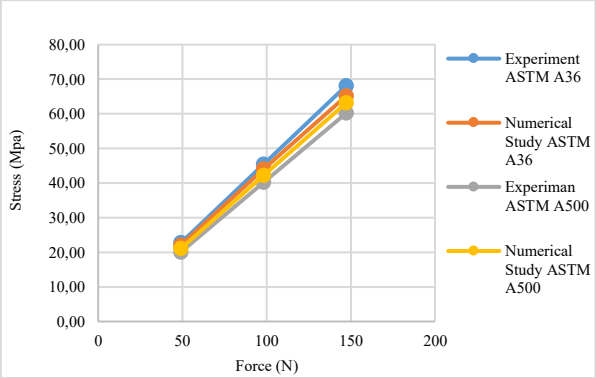

Figure 9. Graph of the relationship between force and stress

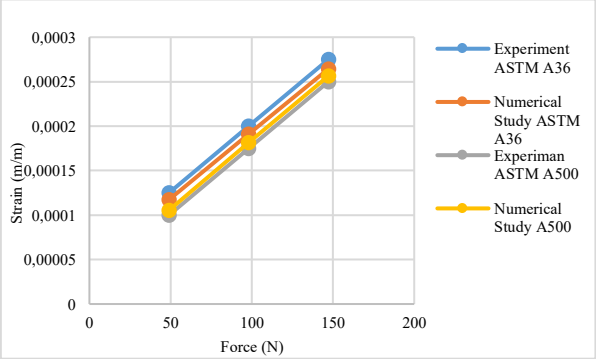

Figure 10. Graph of the relationship between force and strain

Figure 10 shows the stress-strain relationship for ASTM A36 and ASTM A500 based on experimental and numerical results. ASTM A500 consistently exhibits lower strain. At a load of 15 kg (147.15 N), the experimental strain for ASTM A36 is 0.000275 m and for ASTM A500 is 0.00025 m. Numerical results show a strain of 0.00026434 m for A36 and 0.00025642 m for A500. This indicates that ASTM A500 is stiffer because it has a higher modulus of elasticity. Both curves are linear and consistent, proving that the numerical model used is valid

Clean Energy and Smart Technology
Volume 04, Number 02, April 2026
DOI : https://doi.org/10.58641/
e-ISSN : 2964-2647

and highly suitable as a predictive tool in the engineering structural design process, especially for applications requiring accuracy, efficiency, and resistance to deformation due to loading. Thus, the selection of the appropriate material based on numerical analysis can improve the overall performance and reliability of the structure.

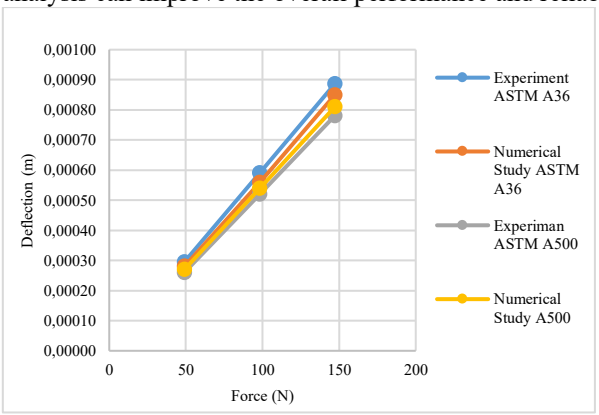

Figure 11. Graph of the relationship between force and deflection

Figure 11 shows the force-deflection relationship for ASTM A36 and ASTM A500 materials, based on experimental and simulation results. Deflection increases linearly in both materials, indicating elastic behavior. ASTM A500 exhibits lower deflection at all loads; for example, at 147.15 N (15 kg), the experimental deflection of ASTM A36 reaches 0.00089 m, while that of ASTM A500 is only 0.00078 m. Numerical results show a similar trend: 0.00084958 m for A36 and 0.00080954 m for A500. This indicates that ASTM A500 is stiffer, making it suitable for precision structures such as AGVs.

The error margins between experimental and numerical results were also low: for A36, the errors were 5.22% (5 kg), 5.26% (10 kg), and 4.13% (15 kg); whereas A500 exhibited smaller and more stable errors, namely 3.81%, 3.77%, and 3.74%. These results demonstrate the validity of the numerical model and the superiority of ASTM A500 in terms of stiffness and geometric stability, making it more recommended for AGV structural applications.

Simulation results for structures using ASTM A36 and ASTM A500 materials show that the safety factor decreases as the load increases, with a significant difference in performance between the two. For ASTM A36 material, the minimum safety factor was recorded at 13.5793 for a 5 kg load, decreasing to 6.3578 at a 10 kg load, and further dropping to 1.9671 under a 15 kg load, approaching the minimum safe limit (safety factor = 1). Meanwhile, ASTM A500 material demonstrates superior performance with a minimum safety factor of 14.7679 at a 5 kg load, 8.1999 at a 10 kg load, and remains at 2.7145 when subjected to a 15 kg load. This comparison shows that ASTM A500 can withstand greater loads at lower stress levels relative to its strength limit compared to ASTM A36.

In terms of efficiency, ASTM A500 can be said to be structurally superior. This is because the material has a higher yield strength, so it can provide a higher safety factor under the same load. This advantage allows for lighter structural design without sacrificing strength, meaning material usage can be more economical. Additionally, the higher safety factor provides an extra safety margin against the risk of failure. Therefore, when considering performance and safety, ASTM A500 is a more optimal and efficient choice compared to ASTM A36, provided that its cost and availability align with the technical specifications.

Recent studies on robotic and vehicle chassis design confirm that the combination of experimental testing and finite element analysis is an effective approach for evaluating structural performance. In this study, the grid independence test shows that the numerical model reached a stable condition, as indicated by the small deflection difference between the two finest meshes. The low error between experimental and numerical results also demonstrates that the FEA model is reliable for predicting the structural behavior of the AGV chassis. This finding is consistent with Liu et al. (2026) and Rebhi et al. (2025), who emphasized the importance of mesh validation and experimental verification in improving the accuracy of numerical structural analysis.

The loading test results show that stress, strain, and deflection increase linearly as the load rises from 5 kg to 15 kg, indicating that both ASTM A36 and ASTM A500 remain within the elastic range. Similar results were reported by Kamalaksha et al. (2025) and Yazar et al. (2026), who found that robotic chassis structures must maintain stiffness and dimensional stability under operational loading. In this study, ASTM A500 produces lower deflection

Clean Energy and Smart Technology
Volume 04, Number 02, April 2026
DOI : https://doi.org/10.58641/
e-ISSN : 2964-2647

and a higher safety factor than ASTM A36, showing better resistance to deformation and greater structural reliability.

Overall, the results indicate that ASTM A500 is more suitable for AGV chassis applications because it provides better stiffness, lower deformation, and a higher safety margin under the same loading conditions. This supports recent findings by Rahmatia et al. (2025) and Sucuoglu (2025), which show that material selection and numerical optimization are important factors in improving chassis efficiency, reducing structural risk, and supporting lightweight robotic vehicle design. Therefore, the integration of experimental testing and FEA in this study provides a strong basis for AGV chassis design optimization and material selection.

4. CONCLUSION

The results demonstrate that increasing loads from 5 kg to 15 kg produce a proportional rise in stress, strain, and deflection, indicating a linear elastic structural response for both materials within the tested range. The close agreement between experimental and numerical results confirms the reliability of the Finite Element Analysis (FEA) approach for predicting the structural behavior of compact AGV chassis.

Comparatively, ASTM A500 consistently exhibits lower stress, strain, and deflection, along with a higher safety factor (2.71 at 15 kg load), indicating superior stiffness and geometric stability relative to ASTM A36. This performance difference highlights the significant influence of material selection on the structural efficiency and load-bearing capability of AGV chassis systems.

From an engineering perspective, these findings suggest that the use of ASTM A500 can enhance structural reliability, reduce deformation under operational loads, and improve overall system stability. Furthermore, the validated integration of experimental testing and numerical simulation provides a robust framework for chassis design optimization and material selection, which can be extended to broader applications in lightweight structural and robotic vehicle systems.

5. REFERENCES

Ariyarit, A., Katasila, P., Srinaem, T., & Sukkhanthong, W., (2020) 'The Multi-objective Design Optimization of Automated Guided Vehicles Car Structure using Genetic Algorithms', 2020 IEEE 11th International Conference on Mechanical and Intelligent Manufacturing Technologies (ICMIMT).

Baihaqi, R.A., Pratikno, H. and Hadiwidodo, Y.S. (2020) 'Analisis Sour Corrosion pada Baja ASTM A36 Akibat Pengaruh Asam Sulfat dengan Variasi Temperatur dan Waktu Perendaman di Lingkungan Laut', Jurnal Teknik ITS, 8(2). Available at: https://doi.org/10.12962/j23373539.v8i2.45896.

Bhavikatti, S.S. (2005) Finite Element Analysis. 2nd edn. New Delhi: New Age International Publishers. Available at: https://www.newagepublishers.com/ (Accessed: 10 January 2025).

Haryanto, I. Surya, D. I., & Sudarto, J. (2022) Evaluasi Rancangan Frame Automatic Guided Vehicle (AGV) Dengan Roda Mecanum Menggunakan Metode Elemen Hingga, Jurnal Teknik Mesin S-1.

Kamalaksha, S. A., Kumar, A., Marneni, R., Ahmad, K. A., Singh, S., & Dol, S. S. (2025). *Fluid-dynamic and structural optimization of a suction-enabled autonomous grass-cutter robot*. Results in Engineering. doi: 10.1016/j.rineng.2025.106445.

Kresna, R., Suprapto, N. and Nendra Wibawa, L.A. (2021) 'Desain dan Analisis Tegangan Rangka Alat Simulasi Pergerakan Kendali Terbang Menggunakan Metode Elemen Hingga', 5(1).

Krnjak, A. , Draganjac, I., Bogdan, S., Petrovic, T., Miklic, D., & Kovacic, Z (2015) 'Decentralized control of free ranging AGVs in warehouse environments', in 2015 IEEE International Conference on Robotics and Automation (ICRA). IEEE, pp. 2034–2041. Available at: https://doi.org/10.1109/ICRA.2015.7139465.

Kurniawan, I.E. (2022) 'Analisis Umur Fatik Rangka Penyangga Aileron Flight Control Simulator Berkapasitas 101 kg Di PT MMF', JTM-ITI (Jurnal Teknik Mesin ITI), 6(1), p. 43. Available at: https://doi.org/10.31543/jtm.v6i1.724.

Liu, Y., Gao, X., Li, W., & Tan, J. (2026). *Design and finite element analysis of new energy bus body frame*. Frontiers in Mechanical Engineering, 12, 1775256. doi: 10.3389/fmech.2026.1775256.

Oyekanlu, E.A., Smitch, A. C., Thomas, W.P., Mulroy, G., Hitesh, D., Ramsey, M., Kuhn, D. J., McGhinnis, J.D., Buonavita, S.C., Looper, N. A., NgOma, A., Liu, W., Mcbride, P.G., Shultz, M. G., Cerasi, C. & Sun, D., (2020) 'A review of recent advances in automated guided vehicle technologies: Integration challenges and

research areas for 5G-based smart manufacturing applications', IEEE Access, 8, pp. 202312–202353. Available at: https://doi.org/10.1109/ACCESS.2020.3035729.

Pamosoaji, A.K. Febria Laksana, F., Syamsiro, M., Rina, F., Budiyanto Setyohadi, D., Badruzzaman, A., Novianto, I., Azmi Ainur Bashir, N., Rico Hernawan, S., Megaprastio, B., Khidir, M., & Setiono Bayu Saputra, R. (2023) 'Pendampingan Pengembangan Prototype Automated Guided Vehicles untuk Sektor Pergudangan pada PT Stechoq Robotika Indonesia', Prosiding SENAPAS, 1(1), p. 13. Available at: https://doi.org/https://doi.org/10.24002/senapas.v1i1.7367.

Rahmatia, Mawarani, L. J., & Apriandi, R. (2025). *Numerical study on the material strength of a microcar chassis structure under static and dynamic loads*. Scientific Journal of Mechanical Engineering Kinematika, 10(2), 228–241. doi: 10.20527/sjmekinematika.v10i2.757.

Rebhi, L., Khalfallah, S., Hamel, A., & Essaidi, A. B. (2025). *Design optimization of a four-wheeled robot chassis frame based on artificial neural network*. Proceedings of the Institution of Mechanical Engineers, Part C: Journal of Mechanical Engineering Science, 239(12), 4756–4773. doi: 10.1177/09544062251316755.

Setiawan, F.B. Muntaha, I., Pratomo, L. H., & Riyadi, S. (2023) 'Pattern Recognition on Automated Guided Vehicles Two Wheel Drive (AGV 2WD) Robot for Location Detection Based on Raspberry Pi 4 Model B', Sinkron, 8(1), pp. 338–347. Available at: https://doi.org/10.33395/sinkron.v8i1.11990.

Sucuoglu, H. S. (2025). *Development of topologically optimized mobile robotic system with machine learning-based energy-efficient path planning structure*. Machines, 13(8), 638. doi: 10.3390/machines13080638.

Versteeg, H.K. and Malalasekera, W. (2007) An Introduction to Computational Fluid Dynamics Second Edition. British Library Cataloguing-in-Publication Data. Available at: www.pearsoned.co.uk/versteeg.

Yazar, Z., Coşkun, Y., & Özyılmaz, L. (2026). *Structural analysis and topology optimization of a mobile robot chassis for STEM education*. Adıyaman University Journal of Engineering Sciences, 13, e260107. doi: 10.54365/adyumbd.1775815.